Magnetic ordering and spin-state transition in $R_{0.67}Sr_{0.33}CoO_3$

M. Paraskevopoulos, J. Hemberger, A. Krimmel, and A. Loidl
Experimentalphysik V, Elektronische Korrelationen und Magnetismus, Institut fuer Physik, Universitaet Augsburg, D-86159 Augsburg, Germany

(Received 26 January 2001; published 22 May 2001)

A series of ceramic $R_{0.67}Sr_{0.33}CoO_3$ samples with R=La, Pr, $Pr_{0.5}Nd_{0.5}$, Nd, $Nd_{0.5}Sm_{0.5}$, and Sm have been prepared. We report on detailed structural, electrical, magnetic, and thermodynamic studies. All samples reveal magnetic order, spanning the range from a ferromagnetic metal to a ferrimagnet close to a metal-to-insulator transition. We found a clear correlation between structural properties and resistivity as well as between structure and magnetic exchange interactions. In this context the importance of double exchange is discussed. Heat-capacity experiments show a significant anomaly at the magnetic transition temperature of the La compound only. The samples with magnetic rare-earth ions reveal significant Schottky anomalies at low temperatures and allow for a rough estimate of the crystal-field splittings.

DOI: 10.1103/PhysRevB.63.224416 PACS number(s): 75.50.−y, 71.20.Be, 75.40.−s

I. INTRODUCTION

For trivalent cobalt in $LaCoO_3$ the subtle balance between the crystal-field energy Δ_{cf} and the intra-atomic exchange energy J_{ex} (Hund's coupling) is the precursor of a peculiar spin-state transition observed around 90 K.[1] At the lowest temperatures, Co^{3+} is in a low-spin (LS) configuration $t_{2g}^6 e_g^0$ revealing a nonmagnetic ground state with $S=0$. Upon heating, thermal excitations lead to a gradual population of intermediate spin states (IS) $t_{2g}^5 e_g^1$ with $S=1$.[2,3] At even higher temperatures a metal-insulator transition occurs and most probably the high spin state (HS) $t_{2g}^4 e_g^2$ with $S=2$ is established. Recently in the structurally related $RBaCo_2O_5$ (R=Y, Tb) compounds, a spin-state transition of the Co ions has also been observed.[4,5]

In general the magnetic and electronic properties of ABO_3 perovskite oxides can easily be tuned by modifying the lattice parameters.[6] The crystal symmetry changes from cubic to rhombohedral and subsequently to orthorhombic, depending on the size of the A and B ions. The different lattice distortions are determined by the tolerance factor t, which is defined as $t=(\langle r_A\rangle+\langle r_O\rangle)/[\sqrt{2}(\langle r_B\rangle+\langle r_O\rangle)]$. Here $\langle r_i\rangle$ represents the ionic size of each element in the ABO_3 perovskites.[7] When t is close to 1, the cubic perovskite structure is obtained (e.g., $SrTiO_3$). As t decreases the lattice symmetry transforms to rhombohedral and subsequently to orthorhombic, in which the B-O-B bond angle more and more deviates from 180°. Concomitantly the crystal field (CF) slightly changes at the B site. In most cases this effect can be neglected (e.g., in the manganates). However, in cobalt based perovskites the aforementioned balance between Δ_{cf} and J_{ex} can easily be disturbed, yielding transitions between different electronic configurations. This possibility of inducing and controlling a spin-state transition through structural tuning motivated us to reinvestigate the $R_{1-x}A_xCoO_3$ series (R=rare earth, A=divalent ion) series. In the early work of Jonker and Van Santen[8] it was shown that $La_{1-x}Sr_xCoO_3$ becomes ferromagnetic (FM) for $x\geqslant 0.15$. Recent studies revealed that for Sr concentrations $0.15\leqslant x\leqslant 0.25$ a cluster formation sets in and that true long-range FM order evolves for $x\geqslant 0.3$ only.[9] The same doping dependence occurs when La is substituted by other rare-earth ions.[10–12] In this paper we report on systematic magnetic, electric, and thermodynamic measurements in $R_{0.67}Sr_{0.33}CoO_3$ which clearly indicates magnetic ordering and spin-state transitions as a function of $\langle r_A\rangle$.

II. EXPERIMENTAL DETAILS

The polycrystal specimens were prepared using conventional ceramic techniques. Ultra pure oxide powders were dried, mixed in the appropriate amounts, and were carefully ball-milled to ensure homogeneous samples. The $R_{0.67}Sr_{0.33}CoO_3$ samples have been pressed into pellets and were prepared by heating in air at 1250°C for 120 h and then slowly cooled to room temperature. For practical reasons, when refering to a specific sample, only the R ions are denoted (e.g., $Nd_{0.5}Sm_{0.5}$ holds for $[Nd_{0.5}Sm_{0.5}]_{0.67}Sr_{0.33}CoO_3$). It has been experimentally established that for samples prepared in air, oxygen stoichiometry is prevailed for doping levels up to 50%.[13,14] Hence we assign our samples a nominal oxygen content of 3, although we are aware of possible small deviations from the ideal stoichiometry. Powder-diffraction patterns were collected employing Cu-$K_{\alpha 1}$ radiation at room temperature. All samples revealed the proper perovskite structure with no traces of impurity phases. For R=La the diffraction pattern was indexed on the basis of a hexagonal lattice ($a=5.4424$ Å, $c=13.1380$ Å), although rhombohedral indexing is equivalent. All other samples reveal an orthorhombic structure. The lattice parameters for the orthorhombic samples as a function of average ionic radii $\langle r_A\rangle$ are shown in Figs. 1(a)–(c). Clearly two orthorhombic phases can be distinguished. For $\langle r_A\rangle>1.21$ Å the typical orthorhombic distortion ($a/c>\sqrt{2}$) appears as a consequence of the cooperative buckling of the CoO_6 octahedra. However, for $\langle r_A\rangle<1.21$ Å the ratio a/c becomes almost equal to $\sqrt{2}$ and might signal the onset of additional Jahn-Teller distortions. We note that the parent compounds with heavy rare-earth ions do not show any cooperative long-range Jahn-Teller distortion.[15] However, the possibility of short-length dynamical Jahn-Teller distortions, as reported

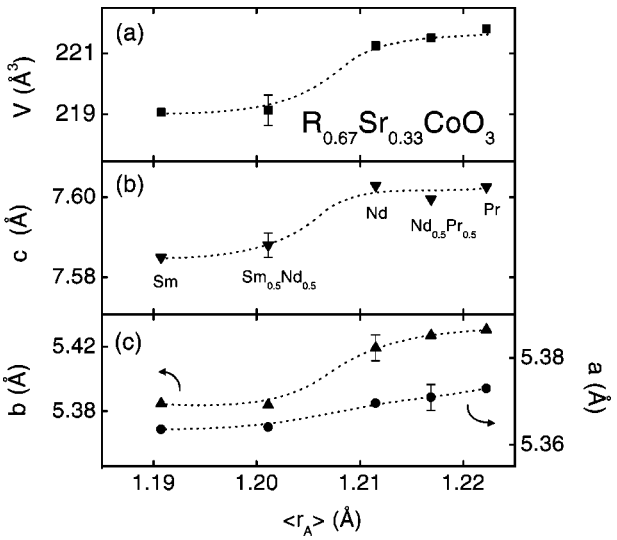

FIG. 1. Orthorhombic lattice parameters for the $R_{0.67}Sr_{0.33}CoO_3$ compounds as a function of $\langle r_A \rangle$. The hexagonal La compound has been omitted. Solid lines are to guide the eye.

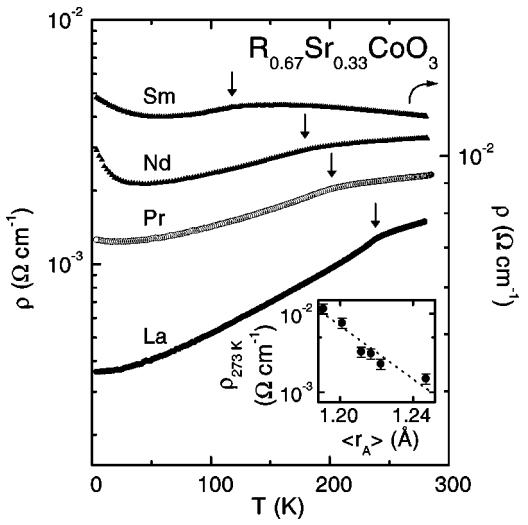

FIG. 2. Temperature dependence of the dc resistivity for R = La, Pr, Nd, and Sm. The inset shows the room-temperature resistivity ρ_{273K} as a function of $\langle r_A \rangle$.

for $La_{1-x}Sr_xCoO_3$ by Louca *et al.*,[16] cannot be excluded. Especially when considering the doped compounds, one has to pay attention to the fact that the intermediate spin states of Co^{3+} ($t_{2g}^5 e_g^1$) and Co^{4+} ($t_{2g}^4 e_g^1$) are both susceptible to Jahn-Teller distortions due to the double degeneracy of the e_g orbitals.

The magnetic susceptibility and magnetization were measured using a dc superconducting quantum interference device magnetometer (0–50 kOe, $1.5 \leqslant T \leqslant 400$ K) and a dc-extraction magnetometer (0–140 kOe, $1.5 \leqslant T \leqslant 300$ K). Resistivity measurements were performed with a standard four-probe method. The heat capacity of the samples was measured using an ac method.

III. RESULTS AND DISCUSSION

A. Electronic properties

The temperature dependence of the dc resistance ρ for R = La, Pr, Nd, and Sm is shown in Fig. 2. The La, Pr, and Nd samples reveal metallic behavior ($d\rho/dT > 0$) above and below T_c. The Sm sample exhibits a weak semiconducting characteristic ($d\rho/dT < 0$) above T_c, and changes slope in the magnetically ordered regime, although it should be noted that the overall temperature dependence is relatively weak. An anomaly at T_c with an increase of the slope $d\rho/dT$ on decreasing temperature can be detected for all samples investigated. This effect probably is due to a freezing out of spin-disorder scattering. One could argue that the increase in conductivity below T_c also indicates the onset of double exchange (DE) interactions, which are known to play a dominant role in the manganate systems. But as we discuss later on, the DE mechanism seems to be only of minor importance in the cobaltites. The Nd and Sm samples show an additional interesting behavior concerning the electronic properties. The resistance shows a pronounced minimum at low temperatures correlated to the observation of a maximum in the magnetization as we discuss in Sec. III B. The room-temperature resistivity strongly increases with decreasing ionic radii $\langle r_A \rangle$ and is enhanced by almost a factor of 10 when $\langle r_A \rangle$ decreases from 1.24 to 1.20 Å (see the inset of Fig. 2). This effect results from an increasing buckling of the CoO_6 octahedra and a concomitant decrease of the charge transfer along the Co-O-Co bonds.

B. Magnetic properties

Figures 3(a)–(d) shows the temperature dependence of the magnetization (left scale) for R = La, Pr, Nd, and Sm. Within the same frame the inverse susceptibility $1/\chi$ is shown vs temperature (right scale). In the paramagnetic re-

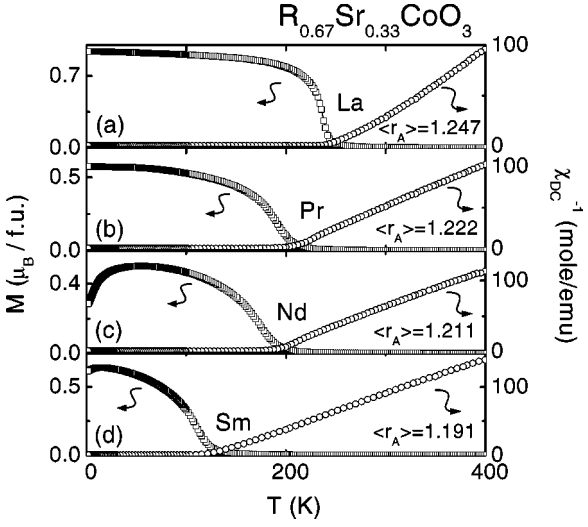

FIG. 3. Temperature dependence of the dc magnetization (left scale) and inverse magnetic susceptibility χ (right scale) for the samples R = La (a), Pr (b), Nd (c), and Sm (d) measured in a field of 10^3 Oe. The average ionic radius $\langle r_A \rangle$ of the A site for each compound is also indicated.

TABLE I. Variation of average ionic radius $\langle r_A \rangle$, paramagnetic Curie-Weiss temperature Θ, ferromagnetic transition temperature T_c, spontaneous magnetization M_s measured at 5 K, and effective magnetic moment p_{eff} (measured and calculated) for various $R_{0.67}Sr_{0.33}CoO_3$ compounds. The most probable corresponding spin state of the Co^{3+} and Co^{4+} ions are also indicated.

R	$\langle r_A \rangle$(Å)	Θ(K)	T_c(K)	$M_s(\mu_B)$	$p_{eff}^{exp}(\mu_B)$	$p_{eff}^{theo}(\mu_B)$	Co^{3+}	Co^{4+}
La	1.2470	263.5	239.0	1.64	3.37	3.21	IS	IS
Pr	1.2222	200.1	192.6	0.88	2.63	2.52	IS	LS
$Pr_{0.5}Nd_{0.5}$	1.2168	187.3	186.2	0.56	2.64	2.52	IS	LS
Nd	1.2115	178.8	173.6	0.37	2.57	2.52	IS	LS
$Nd_{0.5}Sm_{0.5}$	1.2011	152.3	142.4	0.52	2.98	3.21	IS	IS
Sm	1.1907	125.9	112.3	0.55	3.54	3.21	IS	IS

gime all samples obey the Curie-Weiss (CW) law. The paramagnetic CW temperature Θ steadily decreases on decreasing ionic radii of the R ions (Table I). It amounts 263.5 K for $R=$La and decreases to values as low as 112.3 K for the Sm compound. While the almost semiconducting Sm compound exhibits an ideal CW behavior, FM fluctuations show up in the metallic La sample, while for $R=$Pr, $Pr_{0.5}Nd_{0.5}$, and Nd the inverse susceptibility gets suppressed close T_c. The latter behavior most probably indicate the onset of ferrimagnetism.

Below the transition temperature T_c all samples reveal a spontaneous magnetization which becomes minimal for the Nd compound [Figs. 3(a)–(d) and Table I]. The suppression of T_c is closely related to changes in the lattice distortion induced via the reduction of the average radius of the A ion. As $\langle r_A \rangle$ decreases from La to Sm, the hexagonal lattice structure transforms to orthorhombic, in which the Co-O-Co bond angle deviates significantly from 180°, yielding a reduced effective d-d electron transfer via the O $2p$ states.

The results of the analysis of susceptibility and magnetization are summarized in Table I and in Figs. 4(a) and (b).

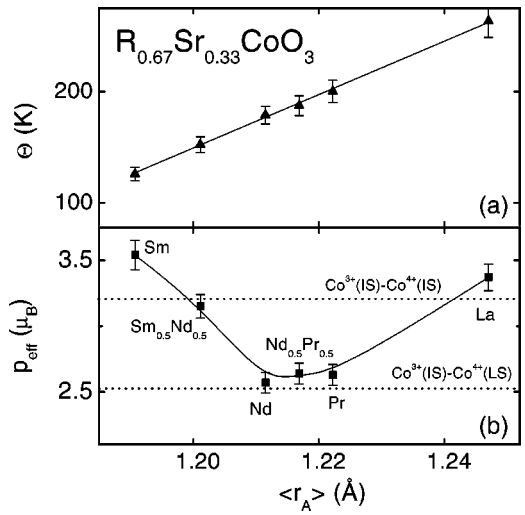

FIG. 4. The paramagnetic Curie temperature Θ (a) and the effective magnetic moment p_{eff} (b) as a function of average ionic radius $\langle r_A \rangle$ for the series $R_{0.67}Sr_{0.33}CoO_3$. In (b) we included theoretical values of p_{eff} for two different electronic configurations of the cobalt ions (dotted lines), which come close to the experimentally observed values.

The paramagnetic Curie-Weiss temperature Θ decreases linearly on decreasing average ionic radii $\langle r_A \rangle$, driven by the same reasons as discussed in the case of T_c [Fig. 4(a)]. To elucidate the spin states of the cobalt ions in the various samples we calculated the effective paramagnetic moments p_{eff} from the linear part of the Curie-Weiss regime by subtracting the contribution of the rare-earth ion [Fig. 4(b) and Table I]. For this calculation tabulated values for the magnetic moments of the R ions were used.[17] Attention has to be paid in the case of the Sm compound, since paramagnetic Sm^{3+} is known not to follow a Curie-Weiss law. We are aware of the fact that some error in our analysis could be caused by a nonlinear behavior of the inverse susceptibility, but we see no other possibility to properly analyze our data. Despite those considerations, it is, however, quite astonishing that the Sm sample shows an almost perfectly linear Curie-Weiss behavior above the magnetic ordering temperature [see Fig. 3(d)]. A minimum of p_{eff} can be observed for $\langle r_A \rangle \sim 1.21$ Å. We also calculated theoretical values of p_{eff} for all compositions assuming a simple ionic spin-only picture, taking the possible spin states (LS, IS, and HS) of the Co^{3+} and Co^{4+} ions into account. We note that all calculations were performed using a Landé factor of $g=2$, despite the fact that measurements made by Bahadur *et al.*[18] revealed a g value close to 1.25 for related materials. Theoretical values for the most probable corresponding spin state of the Co ions are indicated in Table I. For $R=$La, both cobalt species (i.e., Co^{3+} and Co^{4+}) seem to be in an IS state. As discussed later, this conclusion also is supported by field-dependent magnetization measurements. For the Pr, $Pr_{0.5}Nd_{0.5}$, and Nd samples either Co^{3+} or Co^{4+} transforms into a LS state, yielding a reduced p_{eff}. This spin-state transition is triggered by the change in lattice symmetry as observed by replacing La through Pr or Nd. Concomitantly a change in the crystal field makes the LS state more favorable. It is somewhat unexpected that p_{eff} rises again for the $R=Nd_{0.5}Sm_{0.5}$ and Sm compounds. However, this can be understood by taking the structural changes into account which appears for $\langle r_A \rangle < 1.21$ Å (Fig. 1). We already noted that for these compounds $c/a \sim \sqrt{2}$, a fact that indicates the system to be close to an Jahn-Teller (JT) instability. It is generally accepted that polaronic effects can significantly renormalize and enhance the p_{eff} values, especially in the case of JT ions (e.g., Mn^{3+}).[19] As mentioned in Sec. II, this

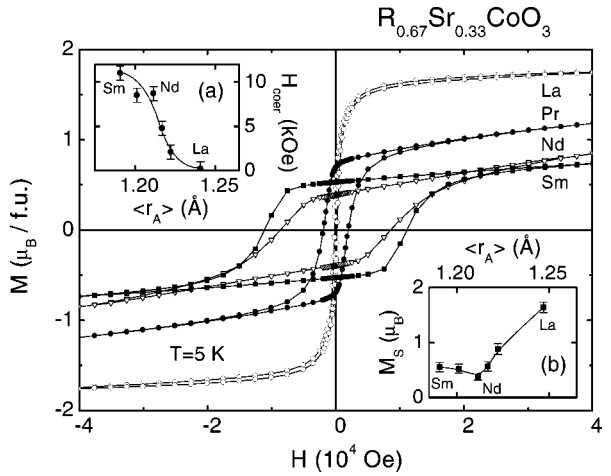

FIG. 5. Field dependence of the magnetization at $T=5$ K for the $R_{0.67}Sr_{0.33}CoO_3$ compounds ($R=$La, Pr, Nd, and Sm). In the insets (a) and (b) the coercive field H_{coer} and the spontaneous magnetization M_s are shown as a function of $\langle r_A \rangle$, respectively.

possibility has to be taken into account when considering IS Co^{3+} ($t_{2g}^5 e_g^1$) and IS Co^{4+} ($t_{2g}^4 e_g^1$) electronic configurations, which are both susceptible to Jahn-Teller distortions of dynamical and static nature. Since charge carries are close to localization in the $Nd_{0.5}Sm_{0.5}$ and Sm samples and are rather itinerant in the La and Pr compounds (see Fig. 2), it is reasonable to assume that polaronic effects due to dynamic JT distortions become more effective for the former compounds, naturally explaining the enhanced p_{eff} values. It is also possible that short-length cooperative JT effects stabilize the IS state for both cobalt species in the samples with $c/a \simeq \sqrt{2}$ as suggested by Louca *et al.*[16]

The low-temperature magnetization behaves rather differently in the various compounds under investigation (Fig. 3, left scale). For an applied magnetic field of $H=10^3$ Oe $La_{0.67}Sr_{0.33}CoO_3$ shows a steep increase of $M(T)$ just below the ferromagnetic ordering temperature and a saturation close to $0.8\mu_B$. The Nd and Sm compounds exhibit a much smaller increase of $M(T)$ and saturation values close to $0.5\mu_B$ (Nd) and $0.6\mu_B$ (Sm) are reached, followed by a decrease of $M(T)$ towards lowest temperatures, a feature which is especially distinct in $Nd_{0.67}Sr_{0.33}CoO_3$. We note that in related systems a glassy behavior at low temperatures has often been reported.[20,21] Considering the ferromagnetic nature of double exchange interactions between Co^{3+}-Co^{4+} and antiferromagnetic superexchange interactions between Co^{3+}-Co^{3+} and Co^{4+}-Co^{4+}, it was suggested that cluster-glass behavior shows up, due to the competition betweeen FM and AFM interactions along with randomness. However, we do not think that in our case a glassy state drives the low-temperature magnetization. We address this issue in more detail at the end of this section.

Hysteresis measurements taken for various samples at $T=5$ K are plotted in Fig. 5. We note that no metamagnetic transitions or other anomalies have been observed for $M(H)$ in fields up to 140 kOe. In the insets the coercive field H_{coer} (a) and the spontaneous magnetization M_s (b) vs $\langle r_A \rangle$ are shown for all compounds. For smaller ionic radii larger coercive fields can be seen [inset (a) of Fig. 5]. This effect most probably is driven by an enhanced magnetic anisotropy induced through the spin-orbit coupling of the rare-earth ions as already discussed by several authors.[11,12] At 5 K the value of the spontaneous magnetization M_s decreases from La to Nd, reveals a minimum for $R=$Nd, and becomes almost constant for smaller ionic radii [inset (b) of Fig. 5]. In the La compound the ordered moment agrees quite well with the expected value considering localized magnetic moments. In fact, the saturated magnetic moment for the La sample is in reasonable agreement with the value reported from neutron-diffraction experiments.[9,22] In the others samples, the ordered magnetic moments deduced from the $M(H)$ curves are significantly smaller than predicted from a simple ionic picture. This behavior is opposite to what has been observed in manganates systems, where the ionic picture worked rather well.[19] In the cobalt compounds under consideration the formation of a narrow σ^* band evolving the Co e_g states calls for an itinerant electron description. The origin of ferromagnetism in cobaltites is still controversial although many authors proposed a double exchange (DE) mechanism.[9] The DE mechanism was initially introduced by Zener to explain the simultaneous occurrence of ferromagnetism and metallic conductivity in the manganates.[23] However, there are several evidences that a simple DE picture cannot hold for the FM state in the cobaltites. First, the essential ingredient of the DE mechanism, a strong Hund's coupling, is absent for the cobalt ions. This is primarily because of the lack of a half filled t_{2g} band which is neccessary for a strong J_{ex}. It is questionable whether DE can drive such a system ferromagnetic. A second evidence comes from the fact that unlike in the manganates, no intimate coupling between ferromagnetism and metallic behavior is present in the cobalt series. One would expect a similar behavior of the conductivity at T_c as has been observed in the manganates. The lack of strong discontinuities in the transport properties at T_c (the resistivity reveals a metallic behavior even for $T>T_c$) and also the absence of colossal magnetoresistance effects call for an alternative explanation (band magnetism).

Figure 6 shows the temperature dependence of the coercitive field H_{coer} (a) and the remanent magnetization M_{rem} (b) for $Nd_{0.67}Sr_{0.33}CoO_3$. H_{coer} exponentially increases upon decreasing temperature reaching values up to 8 kOe. This fact makes zero-field-cooled (ZFC) measurements very difficult to interpret. Even a very small remanent field freezes the spins in and can easily lead to wrong conclusions. Often the splitting of the ZFC and field-cooled (FC) branch of dc magnetization is due to this effect and not driven by spin-glass behavior. Finally the temperature dependence of M_{rem} qualitatively follows the $M(T)$ curve (see Fig. 3).

We now focus on the low-temperature properties of the Nd sample. For $T=50$ K the magnetization starts to decrease again. The same behavior has also been observed for $Pr_{0.5}Nd_{0.5}$, $Nd_{0.5}Sm_{0.5}$, and Sm. In order to study the role of the rare-earth ion we prepared a number of samples with identical $\langle r_A \rangle$ as for the Nd compound. The temperature dependences of the magnetization for these samples are shown in Fig. 7. It can be clearly seen that the ferromagnetic transition temperature T_c remains almost constant. This nicely

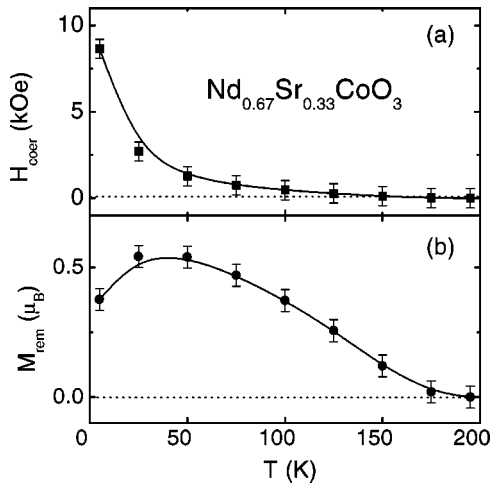

FIG. 6. Temperature dependence of the coercive field H_{coer} (a) and the remanent magnetization M_{rem} (b) for $Nd_{0.67}Sr_{0.33}CoO_3$.

confirms the conclusion that T_c is a function of $\langle r_A \rangle$ only and that in these compounds the structural fine tuning works very well. However, the low-temperature transition accompanied with a reduction in M which clearly is observed in the Nd compound, can hardly be detected in $La_{0.37}Sm_{0.63}$ and is almost absent for $Pr_{0.66}Sm_{0.34}$. This points out that this feature is not related to structural changes. A possible explanation of a decreasing magnetization certainly is an spontaneous antiferromagnetic (AF) order of the Nd^{3+} ions. However in undoped $NdCoO_3$ the Nd^{3+} ions order antiferromagnetically at $T_N \simeq 1$ K while the Co^{3+} ions remain paramagnetic.[24,25] It is straightforward to assume that the magnetic interactions between Nd^{3+} ions in $Nd_{0.67}Sr_{0.33}CoO_3$ remain weak. In a forthcoming paper we will present neutron-scattering data, which reveal that the reduced magnetization at low temperatures is due to a ferrimagnetic ordering of the Nd magnetic sublattice mainly induced via the ordered Co moments.[26] In

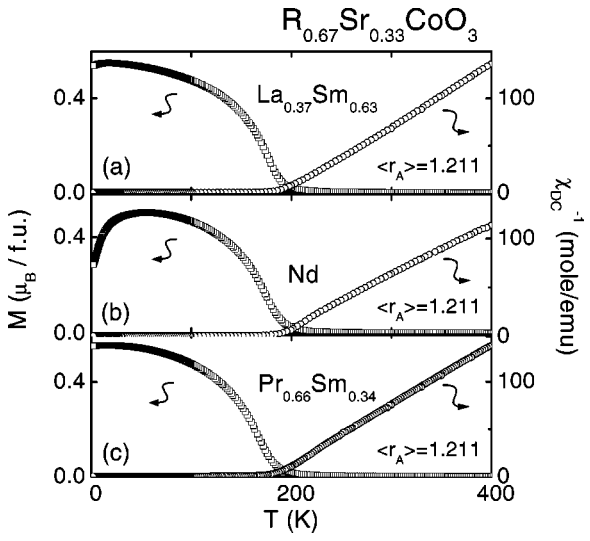

FIG. 7. Temperature dependence of the dc magnetization (left scale) and inverse magnetic susceptibility χ (right scale) for the samples R=LaSm, Nd, and PrSm (a), (b), and (c), respectively, measured in a field of 10^3 Oe.

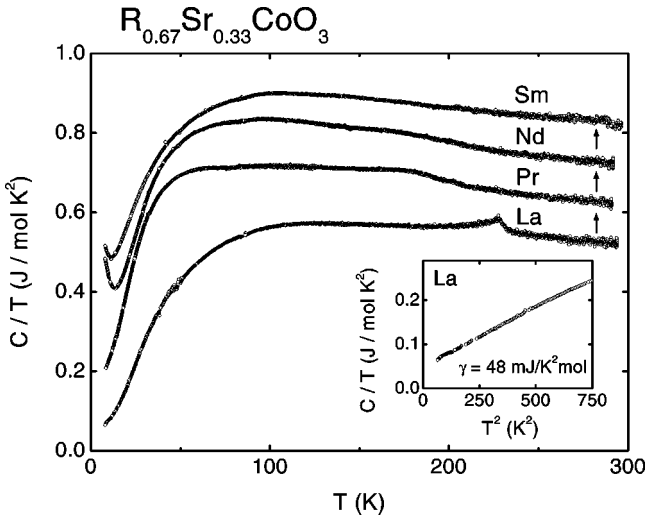

FIG. 8. Specific heat for the samples R=La, Pr, Nd, and Sm. The curves are shifted in steps of 0.1 J/mol K^2. A sharp transition associated with a pronounced peak has only been observed for R=La. For the other samples the anomaly at T_c is smeared out. In the inset we plot C/T vs T^2 for the La sample.

order to explain the reduced values of the low-temperature magnetization, we assume that the Nd moments are aligned antiparallel to the field created by the Co moments. Hence some antiferromagnetic Nd-Co coupling must be invoked. Recently ferrimagnetism has been reported for $Gd_{0.67}Ca_{0.33}MnO_3$.[27] The authors suggested a molecular-field model with a ferromagnetic manganese sublattice antiparallel to the gadolinium sublattice and we think that the very same considerations apply also in the present system.

C. Specific heat

Figure 8 shows the specific heat for $R_{0.67}Sr_{0.33}CoO_3$ (R=La, Pr, Nd, Sm). At the moment only the data down to 8 K are available. A sharp transition associated with a pronounced peak at the ferromagnetic transition temperature has only been observed for R=La. For the other samples the anomaly at T_c is smeared out. It is noticable that the data in the vicinity of the magnetic phase transition reveal very small values for the entropy changes associated with the Co ordering. An estimate, as obtained by integrating the area between the measured curve and a smooth background curve passing through the temperature range from 180 to 250 K only gives $\sim$10% of the expected entropy. Similar observations in related materials (e.g., manganates) have been reported by other groups.[28–30] The inset of Fig. 8 shows C/T vs T^2 for the La sample. Since the La compound is metallic a linear electronic contribution to the specific heat has been expected. A linear extrapolation of $C/T \rightarrow 0$ K yields a Sommerfeld coefficient $\gamma = 47.8$ mJ/K^2 mol. This γ value is two times larger than in $Nd_{0.67}Sr_{0.33}MnO_3$,[30] and 16 times larger than in $La_{0.7}Sr_{0.3}MnO_3$.[31] As already discussed by Gordon *et al.*[30] this linear term probably is mainly magnetic in origin and similar contributions have also been observed in the nonmetallic $NdCu_2O_4$.[32] For the other samples contri-

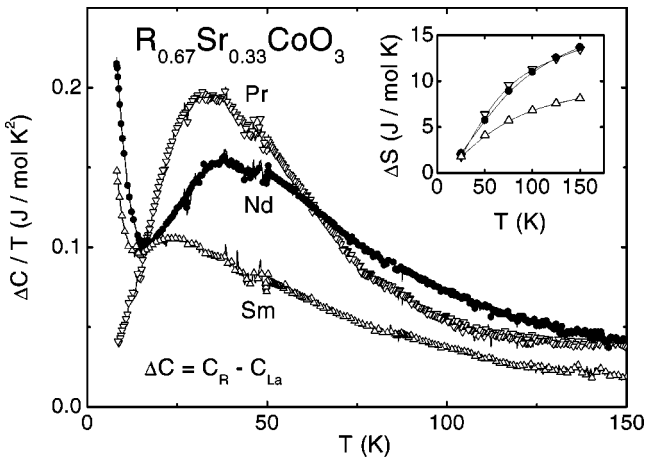

FIG. 9. Schottky anomalies for $R=$Pr, Nd, and Sm obtained by taking the difference between the R curve and the La one. In the inset we show the calculated entropy obtained by integrating the curves shown in the main frame.

butions due to crystal-field effects of the magnetic rare-earth ions make an analysis of the low-temperature data more complicated.

Figure 9 shows Schottky anomalies for $R=$Pr, Nd, and Sm which have been obtained by substracting the heat capacity of the $La_{0.67}Sr_{0.33}CoO_3$ from that observed for the other rare-earth compounds. Schottky-type anomalies have been found in all three compounds investigated with maxima close to 30 K (Pr), 35 K (Nd), and 20 K (Sm). However, for the latter two compounds a further Schottky anomaly appears toward lower temperatures. We also calculated the entropy from these curves by integrating the C/T curves from 5 to 150 K in steps of 25 K. The upper limit is given by the ferromagnetic transition temperatures of the samples, since only the contributions from rare-earth ions should be taken into account and not the ones resulting from the ordering of the cobalt moments. Theoretically values of $S=0.67R\ln(2J+1)$ J/mol K (Pr: 12.2, Nd: 12.8, and Sm: 10) are expected. The discrepancy between measured and calculated values can be understood if one considers that the analysis was limited by a lower bound of 5 K and that especially for Nd and Sm contributions are expected to show up below this temperature as is evident from Fig. 9. Errors could also rise up from the fact that the ferromagnetic order of the cobalt moments may be not the same throughout the whole series, i.e., the polarization of the spin-up and spin-down bands may differ. Measurement of the low-T specific heat have to be performed to arrive at final conclusions.

IV. CONCLUSIONS

We have presented detailed magnetic susceptibility, magnetization, electrical resistivity, and heat-capacity results on the doped rare-earth cobaltites $R_{0.67}Sr_{0.33}CoO_3$. We would like to recall that in the doped manganates of similar composition, large magnetoresistance effects are apparent when the systems passes from an insulating paramagnetic to a metallic ferromagnetic state. For these effects the double exchange interactions play a vital role. Depending on the spin state of the cobaltites similar effects were expected. However, it is well established that in these systems the crystal-field energies are of the order of the Hund's coupling making these systems even more complex. In the course of this work polycrystalline samples have been prepared. The lattice constants show a steplike increase as the average ionic radii of the rare-earth ions increase. We interpret this observation as a result from an increasing importance of Jahn-Teller distortions for larger ionic radii. All samples reveal a metallic character, with the La compound being a rather good metal and the Sm compound being on the borderline of a metal-to-insulator transition. We established a clear correlation between the ionic radii and metallicity. In addition, another clear correlation exits between the magnetic ordering temperatures and the ionic radii. From the effective paramagnetic moments we give an estimate of the spin states of the compounds investigated. We conclude that Co^{3+} always is in an intermediate spin state, while Co^{4+} reveals a low spin state for $R=$Pr and Nd. The La compound exhibits a pure ferromagnetic ground state, while in the systems doped with magnetic rare-earth ions we find indications for ferrimagnetism with the spins of the cobalt and the rare-earth ions pointing in opposite directions and yielding a reduction of the bulk moment at low temperatures. These effects are strongest in the Nd compound. The decrease in the mangetization due to a strong increase of the ordered rare-earth moment aligned antiferromagnetically to the Co ions is correlated with a significant increase of the resistivity. At present we have no explanation for this behavior. From heat-capacity measurements we find a linear electronic contribution to the specific heat with a Sommerfeld coeffient $\gamma=47.8$ mJ/K^2 mol. This large γ value can only be explained taking magnetic contributions into account. The samples containing magnetic rare-earth ions reveal clear Schottky-type anomalies due to crystal-field effects.

ACKNOWLEDGMENTS

This research was supported by the BMBF via Contract No. VDI/EKM 13N6917 and partly by the Deutsche Forschungsgemeinschaft via SFB 484 (Augsburg).

[1] P.M. Raccah and J.B. Goodenough, Phys. Rev. **155**, 932 (1967).
[2] M.A. Korotin, S.Yu. Ezhov, I.V. Solovyev, V.I. Anisimov, D.I. Khomskii, and S.G. Sawatzky, Phys. Rev. B **54**, 5309 (1996).
[3] T. Saitoh, T. Mizokawa, A. Fujimori, M. Abbate, Y. Takeda, and M. Takano, Phys. Rev. B **55**, 4257 (1997).
[4] T. Vogt, P.M. Woodward, P. Karen, B.A. Hunter, P. Henning, and A.R. Moodenbaugh, Phys. Rev. Lett. **84**, 2969 (2000).
[5] Y. Moritomo, T. Akimoto, M. Takeo, A. Machida, E. Nishibori, M. Takata, M. Sakata, K. Ohoyama, and A. Nakamura, Phys. Rev. B **61**, R13 325 (2000).
[6] J.B. Goodenough, *Magnetism and the Chemical Bond* (Interscience, New York, 1963).

[7] In the present study we use ionic radii from the tabulated values of R.D. Shannon, Acta Crystallogr., Sect. A: Cryst. Phys., Diffr., Theor. Gen. Crystallogr. **A32**, 751 (1976). We note that the small size of the *A*-site ions (i.e., La, Pr, Nd, Sr, etc.) leads to a cooperative tilting of the CoO_6 octahedra, reducing the effective coordination number from 12 to 9 for these ions.
[8] G.H. Jonker and J.H. van Santen, Physica (Amsterdam) **19**, 120 (1953).
[9] R. Caciuffo, D. Rinaldi, G. Barucca, J. Mira, J. Rivas, M.A. Senaris-Rodriguez, P.G. Radaelli, D. Fiorani, and J.B. Goodenough, Phys. Rev. B **59**, 1068 (1999).
[10] C.N.R. Rao, O. Parkash, D. Bahadur, P. Ganuly, and S. Nagabhushana, J. Solid State Chem. **22**, 353 (1977).
[11] R. Ganguly, I.K. Gopalakrishnan, and J.V. Yakhmi, Physica B **271**, 116 (1999).
[12] A. Fondado, J. Mira, J. Rivas, C. Rey, M.P. Breijo, and M.A. Senaris-Rodriguez, J. Appl. Phys. **87**, 5612 (2000).
[13] A. Mineshinge, M. Inaba, T. Yao, Z. Ogumi, K. Kikuchi, and M. Kawase, J. Solid State Chem. **121**, 423 (1996).
[14] H.W. Brinks, H. Fjellvag, A. Kjekshus, and B.C. Hauback, J. Solid State Chem. **147**, 464 (1999).
[15] X. Liu and C.T. Prewitt, J. Phys. Chem. Solids **52**, 441 (1991).
[16] D. Louca, J.L. Sarrao, J.D. Thompson, H. Roeder, and G.H. Kwei, Phys. Rev. B **60**, 10 378 (1999).
[17] Charles Kittel, *Introduction to Solid State Physics*, 7th ed. (Academic, New York, 1998).
[18] D. Bahadur, S. Kollali, C.N.R. Rao, M.J. Patni, and C.M. Srivastava, J. Phys. Chem. Solids **40**, 981 (1979).
[19] M. Paraskevopoulos, F. Mayr, J. Hemberger, A. Loidl, R. Heichele, D. Maurer, V. Mueller, A. Mukhin, and A. Balbashow, J. Phys.: Condens. Matter **12**, 3993 (2000), and references therein.
[20] M. Itoh, I. Natori, S. Kubota, and K. Motoya, J. Phys. Soc. Jpn. **63**, 1486 (1994).
[21] S. Mukherjee, R. Ranganathan, P.S. Anilkumar, and P.A. Joy, Phys. Rev. B **54**, 9267 (1996).
[22] V.G. Sathe, A.V. Pimpale, V. Siruguri, and S.K. Paranjpe, J. Phys.: Condens. Matter **8**, 3889 (1996).
[23] C. Zener, Phys. Rev. **82**, 403 (1951).
[24] I. Plaza, E. Palacios, J. Bartolome, S. Rosenkranz, C. Ritter, and A. Furrer, Physica B **234-236**, 632 (1997).
[25] F. Bartolome, M.D. Kuz'min, J. Bartolome, J. Blasco, J. Garcia, and F. Sapina, Solid State Commun. **91**, 177 (1994).
[26] A. Krimmel, M. Reehuis, M. Paraskevopoulos, and A. Loidl (unpublished).
[27] G.J. Snyder, C.H. Booth, F. Bridges, R. Hiskes, S. DiCarolis, M.R. Beasley, and T.H. Geballe, Phys. Rev. B **55**, 6453 (1997).
[28] J. Tanaka and T. Mitsuhashi, J. Phys. Soc. Jpn. **53**, 24 (1984).
[29] A.P. Ramirez, P. Schiffer, S-W. Cheong, C.H. Chen, W. Bao, T.T.M. Palstra, P.L. Gammel, D.J. Bishop, and B. Zegarsk, Phys. Rev. Lett. **76**, 3188 (1996).
[30] J.E. Gordon, R.A. Fisher, Y.X. Jia, N.E. Phillips, D.A. Wright, and A. Zettl, Phys. Rev. B **59**, 127 (1999).
[31] B.F. Woodfield, M.L. Wilson, and J.M. Byers, Phys. Rev. Lett. **78**, 3201 (1997).
[32] R.A. Fisher, D.A. Wright, P. Radhakrishna, A.M. Stacy, J.L. Luce, and N.E. Phillips, J. Magn. Magn. Mater. **177-181**, 787 (1998).